The American Journal of Otology
17:859–865 © 1996, The American Journal of Otology, Inc.

Improved and Simplified Methods for Specifying Positions of the Electrode Bands of a Cochlear Implant Array

Lawrence T. Cohen, Jin Xu, *Shi Ang Xu, and Graeme M. Clark

*Department of Otolaryngology, University of Melbourne, and *Australian Hearing Services, Melbourne, Victoria, Australia*

Objective: To develop techniques for measuring the positions of the individual electrodes of a multiple channel cochlear implant and for estimating associated characteristic frequencies.
Background: Information concerning the positions of the individual electrodes of a cochlear implant array is important for analyzing speech perception or psychophysical data and for optimizing speech-processing strategies. This study presents two techniques for obtaining such information from postoperative plain film radiographs.
Methods: A template spiral shape, derived from analysis of the radiographs of 30 cochlear implant patients, is used to obtain measurements of the angular positions of the electrode bands within scala tympani. A research technique measures angular positions and estimates characteristic frequencies for all electrode bands but requires that the positions of two cochlear landmarks and all electrode bands be digitized. A clinical technique provides similar angle and frequency estimates but requires a minimum of information to be extracted visually from the radiograph. The lateral positions of the bands are estimated, in the research technique, using mean outer and inner wall functions obtained from 11 Silastic molds of scala tympani.
Results: The mean position of the implanted array relative to the mean scala tympani outer wall function was consistent with published histologic observations of implanted temporal bones. Measured angles did not vary greatly with experimenter or with rotation of the cochlea relative to the radiographic beam by up to 20°.
Conclusions: The techniques described allow, principally, measurement of the longitudinal positions of the bands of a cochlear implant in scala tympani and estimation of corresponding characteristic frequencies. **Key Words:** Cochlear implant array—Electrode bands—Radiology.
Am J Otol **17**:859–865, 1996.

Precise specification of the positions of the individual electrode bands of a multichannel cochlear implant is important for several reasons. In studies of patient speech performance and psychophysics, it is desirable to quantify individual electrode insertion depth as one of the variables. This study arose primarily from that need. Speech-processing strategies may require such data for the optimum presentation of place information. Furthermore, postoperative slippage of the electrode array may be detected. Marsh et al. (1) described a technique for estimating electrode position from analysis of plain film radiographs. The two methods to be described are extensions of their approach and are intended, primarily, to provide information on the longitudinal position of the electrode bands along the scala tympani. However, one method also gives useful information on the lateral position of the bands. It also estimates the position of the round window (RW) and the point of entry through a cochleostomy.

Recent developments in three-dimensional (3-D) reconstruction from spiral computed tomographic (CT) scans show great promise for the visualization of cochlear structures (2). However, the present simpler and more generally applicable techniques, although more limited in scope, allow the extraction of detailed information concerning electrode position. Although the methods presented use 2-D projections, the errors introduced for normal insertions are small. Kawano et al. (3) calculated the length of the human organ of Corti both from 3-D reconstruction and from reconstruction of 2-D projection onto an axial plane at right angles to the modiolar axis. They found that the latter gave an estimate on average 2.6% less than the former. For some other species a 2-D projection may introduce greater errors (4), although it has been shown to result in an error of only 2.8% in the cat (5).

Marsh et al. (1) observed that electrode position may be more usefully specified in terms of angle than length. The present methods calculate angle, although length information is implicit. The use of angle facilitates the

Address correspondence and reprint requests to Dr. Lawrence T. Cohen, Department of Otolaryngology, University of Melbourne, 384-388 Albert Street, East Melbourne, Victoria 3002, Australia.

comparison of data for electrode arrays that follow different intracochlear trajectories. For example, one array might follow the outer wall of the scala tympani, whereas another might follow the inner wall. Furthermore, cochleas differ in diameter, and, as is indicated by our data, there is a significant difference between mean diameters of male and female cochleas. On the assumption that cochleas of different diameters have similar total angles, equal insertion lengths would result not only in different angular positions (insertion angles) for the individual electrode bands, but in different characteristic frequencies.

The method of Marsh et al. (1) involved the analysis of a patient radiograph taken using a modified Stenver's view (cochlear view) (6). Two anatomic features were identified, corresponding to the apex of the superior semicircular canal (SSC) and the mid-point of the vestibule (V) (Fig. 1). A line drawn through the points marking these features served as a reference line for analysis of the radiograph. They observed that such a line passed close to the RW. Further lines were drawn, tangential to the radiographic image of the electrode spiral and either parallel to or at right angles to the initial reference line. The center of the spiral was taken to be midway between both the horizontal tangent lines and the vertical tangent lines. This construction enabled the cochlea to be divided into quadrants, and the position of an electrode band to be specified in terms of quadrant and approximate angle within a quadrant.

Although this method is useful, it has disadvantages in terms of accuracy and convenience. Taking the spiral center to be midway between tangent lines introduces a systematic error that would substantially impair the accuracy of angle estimates. Furthermore, if the array insertion was shallow, it would be difficult to define the center of the spiral. If one were to use the method routinely to estimate the angles of all 22 conducting bands of a Cochlear limited array, the task would prove tedious, arguably deterring clinicians from applying it. The proposed methods address these issues. The first (research) method, which involves the fitting of a template spiral to the digitized positions of the electrode bands (and requires also the positions of SSC and V), provides a more accurate estimate of the center of the spiral and, therefore, more accurate estimates of insertion angles. It also can accommodate, albeit with reduced accuracy, shallow array insertions. The second (clinical) method is derived from the first but is simple and fast enough to be used routinely in the clinical setup of speech processors for cochlear implants.

In practice, the orientation of the patient's head during the radiographic procedure may differ somewhat from the ideal of the cochlear view (6). Furthermore, estimates of the positions of SSC and V vary for different observers. In order to assess the variation of calculated insertion angles and RW position with orientation of the cochlea relative to the radiograph and with experimenter, six implanted temporal bones were radiographed in various orientations, and numerical estimates were obtained independently by three experimenters.

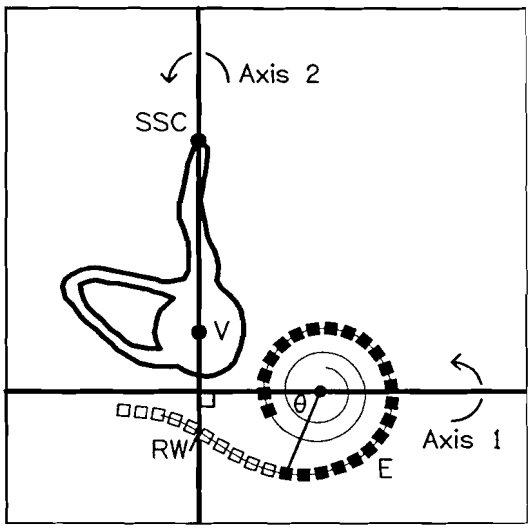

FIG. 1. Diagram of radiograph of implanted cochlea. Outline of vestibular system is shown, with superior semicircular canal (SSC) and vestibule (V). Electrode array is shown inserted through RW. Geometric construction involves drawing reference line through SSC and V, estimation of center of electrode spiral, and construction of a line perpendicular to the reference line and passing through the spiral center. θ is the resulting insertion angle. Also shown are the axes about which six temporal bones were rotat-

MATERIALS AND METHODS

Patient radiographs and temporal bones

Radiographs of 30 patients were selected from the records of the Cochlear Implant Clinic of the Royal Victorian Eye and Ear Hospital (17 male, 13 female). The patients included most of the current volunteers for psychophysics research in the Department of Otolaryngology (University of Melbourne). The radiographs had been taken using the cochlear view (1,6) or similar orientations. The patients were implanted with the standard Cochlear Ltd. receiver–stimulator and electrode array, whereas the temporal bones were implanted with similar arrays. All but two of the patients had been implanted through a cochleostomy.

A total of nine temporal bones were used in the study. Six had been dried and cut away from the apex to expose the scala tympani of the basal and middle turns and some of the apical turn. Electrode arrays were placed in the scala tympani of these, passing through the RW and positioned against the outer wall. The most basal stiffening band was positioned in the RW niche; therefore, the position of the RW was indicated approximately by a point midway between the two most basal stiffening bands. Radiographs were provided (courtesy Martin Donnelly) for an additional three temporal bones, which had been implanted through cochleostomies and in which the position of the RW had been labeled.

Silastic molds of scala tympani

Silastic molds of 11 temporal bones had been made for a previous study (6). Briefly, 11 cadaver adult human temporal bones were fixed and resected to a proper size. The whole bony

labyrinth was maintained intact. The oval window was opened, and the RW membrane was incised using a 30-gauge needle. Silastic MDX-4-4210 was gradually injected with minimum pressure into the scala tympani via the RW. The bony labyrinth with Silastic inside was kept at room temperature for at least 3 days until the Silastic cured. The bony wall of the labyrinth was trimmed away so that an intact Silastic mold could be removed from the labyrinth. The scala tympani part of the Silastic mold was dissected from the rest with ease. The molds were so close to the actual size of the scala tympani that the impression of the membranous labyrinth was clearly visible on them. The spiral ligament was fairly intact when the molds were made.

Radiography of cochlear view

The patient sat in front of a vertical device. The head was rested on the forehead, nose, and zygomatic bone on the implanted side, and the midsaggital plane was adjusted to form an angle of 50° with the plane of the film. The flexion of the neck was adjusted to make the infraorbital plane perpendicular to the film. The central ray was directed to exit from the skull at a point 3.0 cm anterior and 2.0 cm superior to the external auditory meatus at a right angle to the film. Because the electrode array is small, it is important to use macroradiographic techniques.

Image processing techniques

For each patient or temporal bone radiograph, an image of 512 × 512 pixels was captured using a microscope, a video camera (Panasonic WV-CD20), a Data Translation DT2851 frame-grabber card, and an IBM AT-compatible computer. The position of each conducting and stiffening band along the electrode array was then digitized and stored using custom software. In addition, the positions of the apex of the superior semicircular canal, the midpoint of the vestibule, and any relevant markers were stored. The resulting data were processed using further custom software to fit a suitable mathematical spiral expression to the positions of the electrode bands. Images of 11 Silastic molds of scala tympani were captured using similar techniques. Each mold was viewed from the base, the orientation being adjusted manually under the microscope until the axis of the spiral was judged to be parallel to the optical axis. An exponential spiral function was fitted to the outer wall on the image of each of the molds, thereby providing an estimate of the center position. Each image was rotated until the angle of its approximate RW position corresponded to a known mean angle for the RW. The mean outer and inner wall radii were then calculated as functions of angle.

Determination of template spiral for patient radiographs

In order to quantify the positions of the electrode bands of an implanted electrode array, it was useful to determine a spiral template function approximating the shape of the radiographic image of the array. In fitting such a template function to a particular radiograph, both the position and the size of the template would be adjusted. The center position of the fitted template spiral, approximating the modiolus, would be the point about which angles would be measured. The template should describe well the shape of the array in the region where it is close to or in contact with the outer wall of the scala tympani, say for angle $\theta > 100°$ (Fig. 1), regardless of whether the insertion was through the RW or a cochleostomy. For smaller angles, the template should follow the mean trajectory of an RW insertion, thus indicating the position of the RW.

Variation of electrode angle and RW estimates from study of temporal bone radiographs

In order to study the effects of cochlear orientation on estimates of electrode band insertion angles and RW position, the six temporal bones for which electrode arrays had been placed through the RW were radiographed in different orientations relative to the plane of the radiographic film. The distance of the temporal bone from the film was similar to that of a patient's temporal bone, although magnification was not a critical factor because size could be determined using the known separation between the bands of the array. Each temporal bone was mounted on a specimen dish so that the modiolar axis appeared to be perpendicular to the dish. Radiographs were taken with the specimen dish either parallel to the film or tilted relative to it by angles of ±10° and ±20° about one of two perpendicular axes (Fig. 1).

For all temporal bone radiographs (nine different orientations for each of the six bones) template spirals were fitted independently and in random sequence by each of the first three investigators (L.T.C, J.X, S.A.X.) in order to estimate spiral center positions and thus calculate insertion angles and RW positions by the research method. Each experimenter independently chose positions for SSC and vestibule. The computer image of each radiograph had been modified so that they were unable to determine the position of the most basal band of the array (and hence the RW position).

For each temporal bone aligned with modiolus perpendicular to the film, reference angles were calculated for all electrode bands. For this purpose, a mean reference line passed through the mean of the positions for SSC estimated by the three experimenters and through the actual position of the RW, midway between the two most basal stiffening bands. Variation was calculated relative to these reference angles. The position of the RW was measured along the array relative to the mean reference line in an apical direction.

RESULTS

Determination of template spiral for patient radiographs

The outer wall of the scala tympani can be described well by a Cornu spiral (7). However, we found that the shape of the radiographic image of an implanted cochlear limited array could be described well by the following simpler expressions:

$$\theta \geq 100°: R = A \exp(-B\,\theta) \quad (1)$$

$$\theta < 100°: R = C\,[1 - D \log_e(\theta - \theta_0)] \quad (2)$$

where R is the radial distance from the spiral center, θ is the angle in degrees (Fig. 1), and A, B, C, D, and θ_0 are constants.

The optimum value for B (0.001317) was that which resulted in the minimum mean error, among 30 patients, in fitting the exponential function to each of the patient radiographs, for electrode bands with angles of ≥100°. The corresponding mean value for A, the size parameter, was 3.762 mm. It was significantly larger for male than for female cochleas (two-sided t test: $p < 0.05$). For males the mean value was 3.84 mm (SD = 0.19), whereas for females it was 3.66 mm (SD = 0.20). The parameters D and θ_0 (0.12869 and 5.0) were chosen so that,

when the logarithmic function was made equal to the exponential function at 100°, the spiral would pass, on average, through a mean RW position. The mean RW position was determined from analysis of 11 radiographs (nine temporal bones, two patients) for which the RW position was known. In the geometric framework of Fig. 1, the mean angle for the RW position was 13.47°. [The corresponding mean angle for the point of entry of the cochleostomy insertions of this study was approximately 23°, estimated using the mean function for the outer wall of the scala tympani (Fig. 3).] Once the mean template shape had been determined, B, D and θ_0 remained constant. To fit the template to a radiograph, the size parameter A and the spiral center coordinates were adjusted for minimum mean error. The size parameter for the logarithmic function (C) was always such that the radii of the two functions were equal at 100°.

The mean template function is plotted against angle in Fig. 2. Also shown are the mean RW position and the mean radial position for the 28 patients whose arrays were inserted through a cochleostomy. The data for the latter were obtained by fitting the template to the individual patient radiographs and measuring relative to the centers so estimated. The same results are presented on an x-y plot in Fig. 2 (inset), where the spatial relationships can be better appreciated.

Comparison of mean electrode position with scala tympani wall positions estimated from silastic molds

The mean radial position for the 28 patients implanted through a cochleostomy was compared with mean functions for the outer and inner walls of scala tympani, obtained from 11 Silastic molds of scala tympani (Fig. 3). As angle increases beyond ~270°, the curve representing the electrode array passes through the outer wall boundary. This apparent anomaly is explained by the fact that the Silastic outer wall represents approximately the inner boundary of the spiral ligament. The Cochlear Ltd. electrode array is known to penetrate the spiral ligament, making first contact at ~9–14 mm (or ~140–237°) for an RW insertion (8). In the present data, because the radius of the array is at least 0.2 mm, the array would contact the spiral ligament at about 215°.

Variation of electrode angle and RW estimates from study of temporal bone radiographs

Angles of Electrode Bands

Analysis of variance indicated that angular error varied significantly with experimenter [$F(5,146) = 9.50$; $p < 0.001$], with orientation [$F(8,146) = 21.14$; $p < 0.001$], and with temporal bone [$F(5,146) = 55.57$; $p < 0.001$]. However, the mean angular errors differed little between experimenters or with orientation. For the three experimenters, mean errors were –2.83° (LC), –1.10° (SX), and –3.44° (JX). For 0° rotation, the mean error was –1.94°. For rotations of up to 10°, the mean error was –2.26°, whereas for rotations of up to 20°, the mean error was –2.46°. The mean angular error for one bone (bone 10) was –9.69°, which was much larger than for the other bones and resulted from the fact that the experimenters reference lines passed some distance from the RW. These results indicate that estimates of insertion angle did not vary greatly with experimenter or with rotation of the cochlea relative to the radiographic film of up to 20°.

Position of RW

The mean estimated position of the RW was 0.51 mm apical of its true position (SD = 1.07 mm). Analysis of variance indicated that the distance between the RW position and the reference line did not vary significantly with orientation [$F(8,146) = 0.58$; $p = 0.795$] but varied

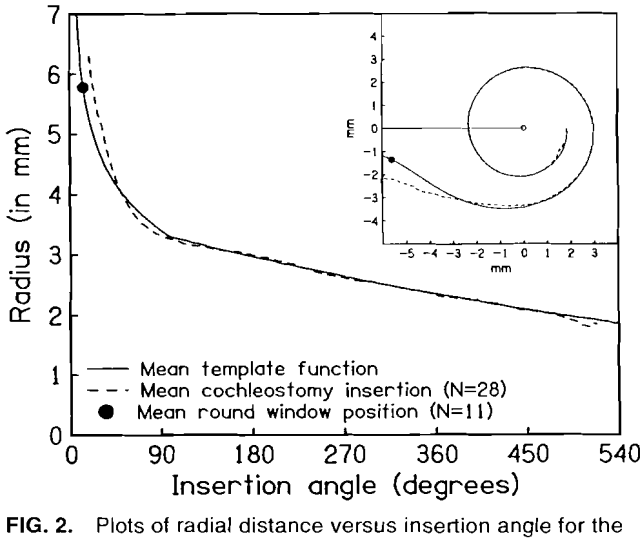

FIG. 2. Plots of radial distance versus insertion angle for the mean template function, mean cochleostomy insertion (28 patients), and mean RW position (nine temporal bones, two patients). **Inset:** Identical data plotted in x-y coordinates.

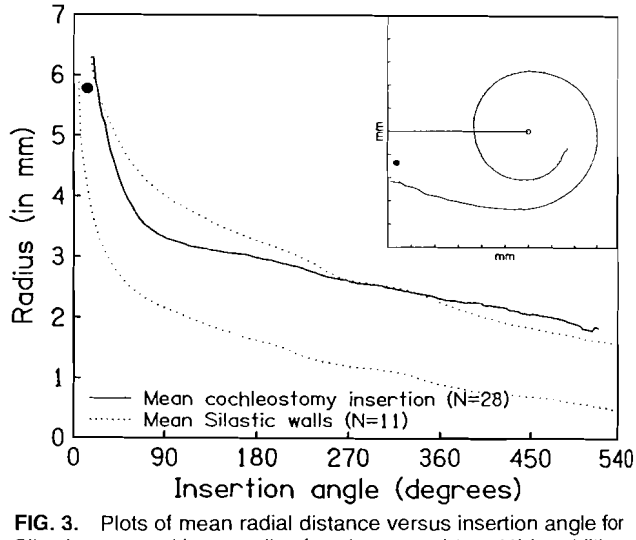

FIG. 3. Plots of mean radial distance versus insertion angle for Silastic outer and inner walls of scala tympani (n = 11) in addition to mean radial distance for cochleostomy insertion (28 patients) and mean RW position (nine temporal bones, two patients). **Inset:** Identical data plotted in x-y coordinates.

with experimenter [$F(5,146) = 12.04$; $p < 0.001$] and with temporal bone [$F(5,146) = 66.47$; $p < 0.001$]. However, the mean distances for the three experimenters did not differ greatly [0.51 mm (LC), 0.22 mm (SX), and 0.79 mm (JX)]. The mean distance for one temporal bone (bone 10) was 2.18 mm, which differed substantially from those for the other bones. If the data for this temporal bone were deleted, the mean distance, over all orientations and experimenters, would become 0.18 mm (SD = 0.67 mm). These results indicate that estimates of RW position did not vary greatly with experimenter or with rotation of the cochlea relative to the radiographic film by up to 20°. They confirm that the reference line passes close to the RW.

Clinical method of angle estimation

A second method was developed for estimating the insertion angles of the bands of a cochlear implant array. This method is simple and clinically applicable and is derived from the research method above. It assumes that the electrode spiral on the radiograph has the form of the template spiral derived above, and that the bands are spaced uniformly. The two unknowns are the size of the spiral and the point on the electrode array where it crosses the reference line drawn through the SSC and V (Fig. 4). The latter is easily found by counting the bands from the basal end of the array to the reference line (5.5 bands at point P0 in Fig. 4). In order to determine the size of the spiral, the number of bands is counted between reference points on the radiographic spiral. The length between the reference points is given by the number of bands multiplied by the band separation (0.75 mm for the Cochlear Ltd. array). The reference points used are the point where the array crosses the reference line (P0 in Fig. 4) and the points where tangents to the spiral are either parallel or perpendicular to the reference line (P1–P6 in Fig. 4). Because the length along the template spiral can also be calculated between corresponding points, the size of the template spiral can be adjusted so that it matches that of the actual radiographic spiral. In Fig. 4, the length would be measured between points P0 and P4, the most apical tangent point (18.83 mm = 25.1 bands × 0.75 mm). Once the size of the template spiral has been determined, angles for all electrode bands can then be calculated from the template spiral. At P0, we know both the angle and the band number on the array. To find the angle for a particular band, we calculate the length around the array from P0 to the band and then calculate the change in angle around the template spiral that would correspond to that length. Angles obtained using the two methods (research and clinical) are in good agreement.

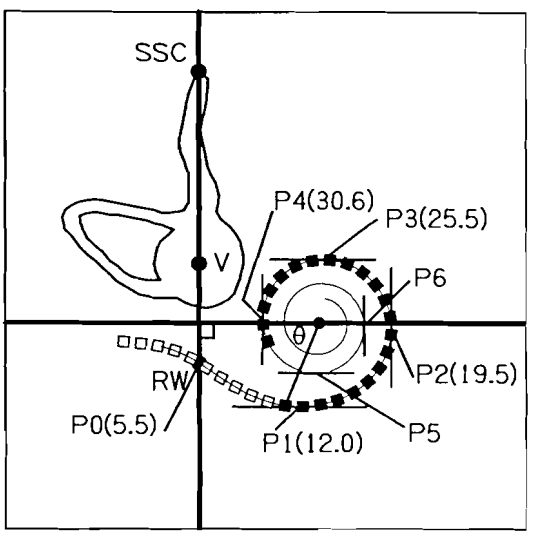

FIG. 4. Clinical method of estimating insertion angles from a radiograph. The electrode bands are counted from the basal end of the array, starting with the most basal stiffening ring. The counts are noted at the points shown, from point 0 where the array cuts the reference line to the most apical tangent point (point 4 in this example). A computer then calculates what spiral size would give these band counts, and estimates the insertion angles for all the bands.

In practice, a clinician would need the radiograph, a light box, and a transparency that was marked with a bold line to represent the reference line and a grid to help visualize the tangents. He or she would superimpose the transparency on the radiograph, align the bold line so that it passed through the SSC and vestibule (Fig. 4), and then count the bands, starting with the most basal stiffening ring, noting the number on crossing the reference line (5.5 in Fig. 4) and the number at the most apical tangent point reached by the array (30.6 in Fig. 4). These band counts would be entered into a computer, which would then perform all other calculations automatically, including angles and associated characteristic frequencies for all electrode bands. This information could then be used to assist in programming the patient's speech processor.

Estimation of characteristic frequencies corresponding to electrode band positions

Insertion angle data can be used to estimate characteristic frequencies corresponding to the bands of an implanted electrode array. The data of Bredberg (9) provide a relationship between angle and percentage length along the organ of Corti, whereas the expression of Greenwood (10) gives frequency as a function of fractional length along the organ of Corti. Therefore, frequency can be expressed as a function of angle, provided the angles measured by Bredberg can be related to the angles used in the present analysis.

The zero angle of Bredberg (9) corresponded to the basal end of the organ of Corti. We used the mean Silastic mold measurements, described above, and data from a 3-D reconstruction of a cochlea (3) to estimate the position of the basal end of the organ of Corti in our framework. The image obtained from the 3-D reconstruction indicated positions of the outer and inner walls of scala tympani and of the organ of Corti. The position of the RW could be estimated in the image, which was scaled and aligned with the present data (Fig. 5). The resulting position of the basal end of the organ of Corti—0° in

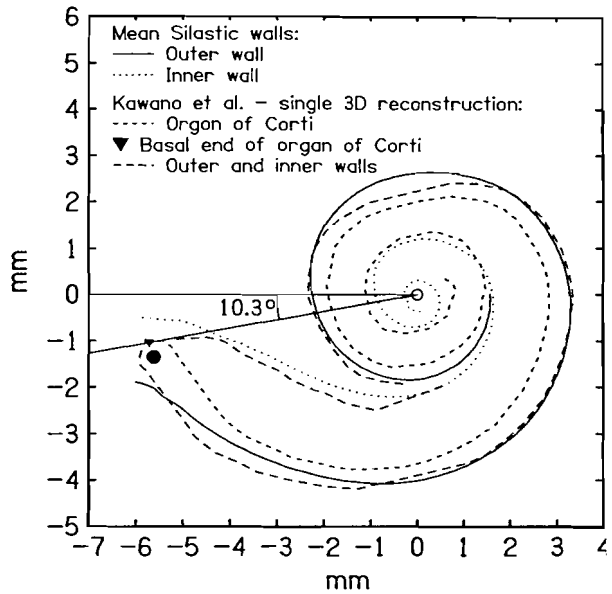

FIG. 5. Superposition of 3-D reconstruction [Kawano et al. (3)] on our mean data for outer and inner walls of scala tympani and RW position (●). The 3-D reconstruction image was scaled and positioned so that it was approximately consistent with our data. This gave an estimate of the angular position of the basal end of the organ of Corti in our geometric framework. Note the basal end of the organ of Corti lies at 10.3° relative to the angular origin in our framework.

Bredberg's (9) scheme—corresponded to an angle of ~10° in the present scheme.

The percentage length versus angle data of Bredberg (9) was smoothed and combined with the expression relating fractional length to frequency given by Greenwood (10). The resulting relationship between angle (in the present scheme) and characteristic frequency is plotted in Fig. 6.

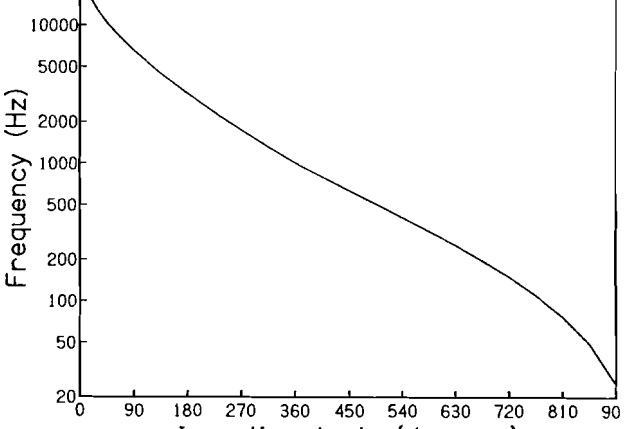

FIG. 6. Characteristic frequency versus insertion angle. Angle was converted to percentage length along the organ of Corti using the data of Bredberg (9). Percentage length was converted to frequency using the expression of Greenwood (10).

DISCUSSION

The techniques described allow researchers and clinicians working with cochlear implant patients to determine insertion angles, and thence characteristic frequencies, for the individual bands of implanted electrode arrays. Angle may be a more appropriate measure of fractional position along the organ of Corti than length because there is some variation in the length of the human cochlear duct (9,11,12). Perhaps more importantly, different electrode arrays may occupy different lateral positions in the scala tympani. As our data for the inner and outer walls of the scala tympani indicate, an array that followed the inner wall would traverse a considerably larger range of angle than would one that followed the outer wall, given equal insertion lengths.

The research method provides useful information on the lateral position of the bands in the scala tympani. When the spiral has been fitted to the band positions, outlines of the mean outer and inner wall positions (ideally appropriate to the sex of the cochlea) can be superimposed on an image of the electrode array, giving a visual impression of the lateral placement of the array. The mean scala wall positions are unlikely to differ greatly from the true wall positions for a radiograph because, among cochleas for a single sex, our data indicate that the size parameter lies within a fairly small range about the mean (~±10%). This technique also allows the position of a cochleostomy to be estimated.

Comparison of the mean trajectory for electrode arrays inserted through cochleostomies and the mean position of the outer wall of the scala tympani, as derived from Silastic molds, corroborated previous findings that the Cochlear Ltd. array penetrates the spiral ligament from about half way around the basal turn (8). This agreement indicates that the lateral position data obtained from the new research method is accurate, at least on average. The research method can be applied readily to arrays that follow different trajectories within the scala tympani, provided their band separations are known, and their shapes are fairly regular and give rise to reasonably accurate estimates of the position of the modiolus. The clinical method also can be adapted to other arrays.

It should be stressed that both research and clinical methods need to be applied with care if satisfactory results are to be obtained. Although our measurements with temporal bones show that estimates of insertion angles do not vary greatly with orientation of the head, good results are obtained only if the radiologic landmarks (SSC and V) are visible on the radiograph. Visibility depends on several factors, including the orientation of the skull and the degree of otosclerosis. The orientation of the patient's head must be fairly close to that prescribed by Xu et al. (6) and as summarized above. The radiographer should follow those guidelines regarding orientation but must be sufficiently experi-

enced to recognize an unsatisfactory radiograph and to adjust the position of the patient's head to obtain a satisfactory result. Of approximately 100 patient radiographs, only two had otosclerosis so severe as to make it impossible to locate the radiologic landmarks. Irregularities in array trajectory (e.g., kinks) result in erroneous angle and frequency estimates unless due allowance is made.

The methods described allow the convenient acquisition of position information for the bands of a cochlear implant array. That information is valuable in speech perception and psychophysical studies, as well as for the optimization of speech-processing strategies. Whitford et al. (13) have shown that improvements in speech perception can result from more nearly matching the spectral frequencies of speech to the characteristic frequencies of the sites of cochlear stimulation. The data provided by the methods are fairly independent of the orientation of the patient's head during the radiographic procedure, subject to the visibility of two radiologic landmarks on the radiograph, and of the judgment of the experimenter in estimating the positions of those landmarks.

Acknowledgment: We thank Julianna M. Silverman for her assistance in obtaining radiographs of electrode arrays implanted in cochlear implant patients and temporal bones, as well as Mr. Martin Donnelly, FRCSI for providing radiographs of implanted temporal bones and for commenting on the manuscript. We thank Dr. Rob Shepherd for his comments on the manuscript. This work was supported by the Human Communication Research Centre, funded by the Australian Research Council, and by the Cooperative Research Centre for Speech and Hearing Research, funded by the Commonwealth Government of Australia.

REFERENCES

1. Marsh MA, Xu J, Blamey PJ, et al. Radiological evaluation of multiple-channel intracochlear implant insertion depth. *Am J Otol* 1993;14:386–91.
2. Skinner MW, Ketten DR, Vannier MW, et al. Determination of the position of Nucleus cochlear implant electrodes in the inner ear. *Am J Otol* 1994;15:644–51.
3. Kawano A, Seldon HL, Clark GM. Computer-aided three-dimensional reconstruction in human cochlear maps: measurement of the lengths of organ of Corti, outer wall, inner wall, and Rosenthal's canal. *Ann Otol Rhinol Laryngol* (in press).
4. Ketten FR, Wartzok D. Three-dimensional reconstructions of the dolphin ear. In: Thomas R, Kastelein R, eds. *Sensory abilities of cetaceans.* New York: Plenum, 1990;81–105.
5. Schuknecht HF. Techniques for study of cochlear function and pathology in experimental animals. *Arch Otolaryngol* 1953;58: 377–97.
6. Xu J, Xu SA, Clark GM, et al. Cochlear view and its application in cochlear implant patients. Presented at the International Cochlear Implant, Speech and Hearing Symposium, Melbourne, Australia, 1994.
7. Spelman FA. Determination of tissue impedances of the inner ear: models and measurements. In: Miller JM, Spelman FA, eds. *Cochlear implants: models of the electrically stimulated ear.* New York: Springer-Verlag, 1989:35–53.
8. Shepherd RK, Clark GM, Pyman BC, et al. Banded intracochlear electrode array: evaluation of insertion trauma in human temporal bones. *Ann Otol Rhinol Laryngol* 1985;94:55–9.
9. Bredberg G. Cellular pattern and nerve supply of the human organ of Corti. *Acta Otolaryngol (Stockh)* 1968;(suppl 236):1–138.
10. Greenwood DD. A cochlear frequency-position function for several species—29 years later. *J Acoust Soc Am* 1990;87:2592–605.
11. Ulehlova L, Voldrich L, Janisch R. Correlative study of sensory cell density and cochlear length in humans. *Hear Res* 1987;28: 149–51.
12. Hardy M. The length of the organ of Corti in man. *Am J Anat* 1938;62:291–311.
13. Whitford LA, Seligman PM, Blamey PJ, et al. Comparison of current speech coding strategies. In: Fraysse B, Deguine O, eds. *Cochlear implants: new perspectives.* Basel: Karger, 1993:85–90.

Author/s:
Cohen, Lawrence T.; XU, JIN; Xu, Shi Ang; Clark, Graeme M.

Title:
Improved and simplified methods for specifying positions of the electrode bands of a cochlear implant array

Date:
1996

Citation:
Cohen, L. T., Xu, J., Xu, S. A., & Clark, G. M. (1996). Improved and simplified methods for specifying positions of the electrode bands of a cochlear implant array. American Journal of Otology, 17, 859-865.